Bioelectrochemistry 107 (2016) 7–13

Contents lists available at ScienceDirect

Bioelectrochemistry

journal homepage: www.elsevier.com/locate/bioelechem

Reduction of low potential electron acceptors requires the CbcL inner membrane cytochrome of *Geobacter sulfurreducens*

Lori Zacharoff [b], Chi Ho Chan [a], Daniel R. Bond [a,c,*]

[a] BioTechnology Institute, University of Minnesota–Twin Cities, Saint Paul, MN 55108, United States
[b] Department of Biochemistry, Molecular Biology, and Biophysics, University of Minnesota–Twin Cities, Saint Paul, MN 55108, United States
[c] Department of Microbiology, University of Minnesota–Twin Cities, Saint Paul, MN 55108, United States

ARTICLE INFO

Article history:
Received 2 April 2015
Received in revised form 23 August 2015
Accepted 24 August 2015
Available online 5 September 2015

Keywords:
Extracellular respiration
Metal reduction
Geobacter
Cytochrome
Microbial electrochemical cell

ABSTRACT

The respiration of metals by the bacterium *Geobacter sulfurreducens* requires electrons generated by metabolism to pass from the interior of the cell to electron acceptors beyond the cell membranes. The *G. sulfurreducens* inner membrane multiheme *c*-type cytochrome ImcH is required for respiration to extracellular electron acceptors with redox potentials greater than −0.1 V vs. SHE, but ImcH is not essential for electron transfer to lower potential acceptors. In contrast, deletion of *cbcL*, encoding an inner membrane protein consisting of *b*-type and multiheme *c*-type cytochrome domains, severely affected reduction of low potential electron acceptors such as Fe(III)-oxides and electrodes poised at −0.1 V vs. SHE. Catalytic cyclic voltammetry of a Δ*cbcL* strain growing on poised electrodes revealed a 50 mV positive shift in driving force required for electron transfer out of the cell. In non-catalytic conditions, low-potential peaks present in wild type biofilms were absent in Δ*cbcL* mutants. Expression of *cbcL in trans* increased growth at low redox potential and restored features to cyclic voltammetry. This evidence supports a model where CbcL is a component of a second electron transfer pathway out of the *G. sulfurreducens* inner membrane that dominates when redox potential is at or below −0.1 V vs. SHE.

1. Introduction

Microorganisms thrive in anoxic environments by coupling oxidation of compounds to the reduction of terminal electron acceptors [1–3]. Due to differences in the redox potential of each electron source and sink, variable amounts of energy are available to bacteria catalyzing this electron flow. For example, every 0.3 V of potential drop between a donor and acceptor releases −58 kJ per two electrons, essentially enough to generate one ATP. In the environment, insoluble metal oxide acceptors span a large range of reduction potentials, from values as low as −0.2 V to as high as +0.5 V vs. standard hydrogen electrode (SHE) [4,5]. This represents an array of thermodynamic opportunities for metal-reducing bacteria, but only if molecular mechanisms have evolved to couple electron transfer to these metal forms via different respiratory pathways.

In microbial electrochemical devices, anode surfaces act as electron acceptors, offering a unique opportunity to test if electron transport chains in different organisms are optimized for growth at particular redox potentials [6–8]. One consistent finding from environmental enrichment experiments is the predominance of *Geobacter* spp. in electrode-reducing biofilms, even though anode potentials are dynamic in fuel cell-like devices, and anode potentials chosen for poised electrode experiments vary over a range greater than 0.5 V. These results suggest that members of the *Geobacter* genus are redox potential "generalists" able to take advantage of the wide range of electron acceptor potentials created by the variety of Fe(III) and Mn(IV) oxides in the environment.

Evidence for redox potential-dependent adaptations can be found in the *Geobacter* j-V cyclic voltammetry response, which measures the rate of electron transfer at different redox potentials. The voltammetric response typical of both pure cultures and enrichments dominated by *Geobacter* relatives does not follow a simple Nernstian relationship for a single one-electron process [9,10]. Recent impedance measurements by Yoho et al. [12], and voltammetry analysis by Rimboud et al. [9], suggests that electron transfer out of *Geobacter*-like bacteria is best described by two to three different pathways, with midpoint potentials near −0.21, −0.15 V and −0.09 V vs. SHE. Consistent with this prediction, deletion of the inner membrane cytochrome gene *imcH* only eliminates growth of *Geobacter sulfurreducens* at redox potentials above −0.1 V vs. SHE, but Δ*imcH* mutants remain able to grow at potentials below this value [13]. These observations lead to the hypothesis that at least one other quinone oxioreductase is active in *Geobacter*, which supports growth of *G. sulfurreducens* at low redox potentials even when *imcH* is deleted [13].

The *G. sulfurreducens* genome encodes at least five other putative quinone oxidoreductase protein complexes, that contain a transmembrane

* Corresponding author at: 140 Gortner Laboratory, 1479 Gortner Ave, Saint Paul, MN 55108, United States.
E-mail address: dbond@umn.edu (D.R. Bond).

http://dx.doi.org/10.1016/j.bioelechem.2015.08.003

b-type diheme domain fused or adjacent to a multiheme *c*-type cytochrome (sometimes annotated as Cbc proteins or clusters) [14,15]. Transcriptomic and proteomic data indicate that some Cbc-like gene clusters are differentially expressed in response to changes in electron acceptor availability or growth in syntrophic co-culture with other strains [16,17]. Transcript abundance of genes encoding Cbc-family proteins is also affected when electrode-reducing communities containing *Geobacteraceae* are exposed to changes in anode potential [18]. Cbc complexes have not been the focus of genetic investigations, even though these complexes share characteristics with other electron transfer proteins, show a high degree of conservation across *Geobacter* genomes, and display dynamic responses in environments where electron acceptor potential is a variable.

This work describes a redox potential-dependent respiratory role for the inner membrane cytochrome CbcL. Deletion of *cbcL* primarily impaired growth with low-potential extracellular electron acceptors, and eliminated an electron transfer process with a midpoint potential of −0.15 V vs. SHE. Electron transfer centered at a higher midpoint potential, near −0.1 V vs. SHE, remained intact in Δ*cbcL* mutants. These results indicate that voltammetry of *G. sulfurreducens* under catalytic conditions is mainly influenced by reactions at the inner membrane rather than the outer surface, consistent with these being the rate-limiting or least-reversible steps. Both CbcL- and ImcH-dependent pathways are present in wild type cells, regardless of growth conditions. However, electron flow appears to switch from the low- to high-potential pathway as external redox potential is raised during a 1 mV/s cyclic voltammogram. Identification of CbcL supports an emerging model of multiple electron transfer pathways in *Geobacter*, where these bacteria rapidly alter their respiratory strategy to take advantage of the different amounts of energy available in extracellular electron acceptors.

2. Materials and methods

2.1. Strains and growth conditions

For each experiment, *G. sulfurreducens* PCA (ATCC 51573) or mutants (described below) were revived from frozen lab stocks by directly plating at 30 °C on 1.5% agar solid medium containing 20 mM acetate donor and 40 mM fumarate acceptor (NBFA medium) containing defined salts [19]. All anaerobic medium was prepared using 80:20 N_2:CO_2 passed over a heated copper column to remove oxygen. Colonies were propagated by picking into 1 mL liquid medium with acetate as the electron donor and fumarate (40 mM) as the electron acceptor, then transferred to medium containing 55 mM Fe(III) oxide, 50 mM Fe(III) citrate or 20 mM Mn(IV) oxide as the electron acceptor for phenotypic experiments. Independent colonies revived from freezer stocks were used for all experiments to avoid repeated transfers in soluble or insoluble electron acceptors that could select for variants.

To determine Fe(III) reduction, 100 μL samples were dissolved in 900 μL 0.5 N HCl, and a FerroZine assay adapted from [20] for the use in 96 well plates was performed. 300 μL of FerroZine solution (2 g FerroZine reagent/L in 100 mM HEPES, pH 7) was added to 50 μL of sample and absorbance at 625 nm was measured. This protocol was adapted for Mn reduction by first dissolving samples in 0.5 N HCl with 4 mM $FeSO_4$, allowing the Fe(II) to reduce remaining Mn(IV), and then proceeding with the steps described above. The extent of Mn reduction could then be calculated by difference.

2.2. Deletion and complementation of cbcL

Strains used for this study are summarized in Table 1. One kb up and downstream of *cbcL* (GSU0274) was amplified and purified. Overlapping PCR was performed, and the resulting product was digested and ligated into the pK18*mobsacB* vector [21], leaving the flanking regions in tandem. This cloned product was sequence verified (UMGC, University of Minnesota) then transformed into a S17-1 *Escherichia coli* donor strain [22]. Wild type *G. sulfurreducens* and *E. coli* mating strains in late exponential phase of growth were applied to filter paper on NBFA agar media in an anaerobic chamber. Twelve hours later a sample was streaked for isolation on NBFA + kanamycin plates to select for plasmid integration. Counter selection on 10% sucrose NBFA selected for recombination events, and colonies were patched on both NBFA and NBFA kanamycin plates. Cells sensitive to kanamycin (indicating plasmid excision) were further screened for complete gene deletion using up and downstream flanking primers (see supplemental Table 1) For complementation, a *G. sulfurreducens* expression vector was generated by cloning the *acpP* (GSU1604) promoter and ribosome binding site to the 5′ region of *cbcL* (GSU0274). Vectors were maintained with 200 μg/mL kanamycin. Before inoculation of reactors, cultures were transferred once into kanamycin-free NBFA to limit the amount of kanamycin carryover into electrochemical reactors, which can reduce final current density.

Table 1
Plasmids and strains.

Strain or plasmid	Description	Source/Reference
Strains		
G. sulfurreducens PCA	Wild Type (ATCC 51573)	Lab collection
Δ*cbcL G. sulfurreducens*	Markerless deletion of *cbcL* gene in wild type *G. sulfurreducens* background	This study
E. coli S17-1	Donor strain for conjugation	Simon, 1983
Plasmids		
pK18mobsacB	Markerless deletion vector	Schafer [21]
pRK2geo2	Vector control and backbone for complementation vector	Lab collection
pcbcL	Complementation vector with constitutive expression of *cbcL*. *cbcL* was cloned into pRK2Geo2.	This study

2.3. Electrochemical analysis

Bioreactors consisted of a polished and sonicated 3 cm^2 graphite electrode (1500 grit), platinum counter electrode and pre-calibrated calomel reference electrode (vs. a laboratory standard) connected to the reactor through a Vycor frit. Bioreactors were constantly stirred, maintained at 30 °C and kept under a constant stream of oxygen-free 80% N_2:20% CO_2 throughout the course of experimentation. Reactors were controlled via potentiostat (VMP, Bio-Logic, Knoxville, TN) running EC-lab software. Bioreactors were poised at either +0.24 V or −0.1 V versus SHE. Experiments were initiated with a 50% (v/v) inoculum of 0.52 OD_{600} cultures entering stationary phase due to electron acceptor limitation.

2.4. Electrochemistry

Catalytic cyclic voltammetry and single turnover experiments were performed by poising the electrode at −0.55 V versus SHE and scanning to a reversal potential of +0.245 V versus SHE at a rate of 1 mV/s, for at least three cycles. Twenty-four hours before single-turnover voltammetry was performed, electrode medium was replaced with acetate free medium, and the electrode was poised as an acceptor to deplete available donors. Cells were washed again in acetate-free buffer immediately before scanning. Cyclic voltammetry was initiated once current was less than 10 μA/cm^2.

2.5. q-RT-PCR

Biofilms were grown on electrodes for 60 h and harvested at 4 °C. Cells were removed by scraping with a sterile, RNase-free pipette tip and collected via centrifugation. RNA was extracted from electrode

grown cells with PureLink system (Life Technologies, Calsbad, CA). cDNA was synthesized using iScript from Bio-Rad (Bio-Rad, Hercules, CA) with random primers as provided. Amplification was observed using SsoAdvanced Universal SYBR green from Bio-Rad per manufacturer's instructions on a Bio-Rad iCycler (supplemental Table 2). Primer efficiencies were calculated from genomic DNA extracted from wild type *G. sulfurreducens* using Wizard Genomic DNA purification kit (Promega, Madison, WI). Samples were normalized to starting RNA levels. The Pfaffl [23] method was used to compare gene expression levels to housekeeping gene levels. Control genes *rpoD* and *proC* did not change relative to each other when compared to high and low potential grown biofilms. The C_T values used to calculate expression ratios were: *cbcL* high potential = 26.1 ± 2.7, and low potential = 24.96 ± 0.69; and *rpoD* high potential 27.18 ± 2.4, and low potential 26.39 ± 0.32.

3. Results and discussion

3.1. Deletion of cbcL primarily affects Fe(III)-oxide reduction

In previous work, deletion of *imcH*, encoding an inner membrane multiheme *c*-type cytochrome, eliminated the ability of *G. sulfurreducens* to reduce acceptors with potentials higher than −0.1 V vs. SHE [13], despite the fact that acetate oxidation linked to reduction of these compounds is energetically favorable. However, the Δ*imcH* strain still reduced acceptors with potentials at or lower than −0.1 V at near wild type rates. These observations led to the hypothesis that *G. sulfurreducens* utilizes different electron transfer pathways, depending upon the redox potential of the terminal electron acceptor.

Inner membrane respiratory proteins such as hydrogenases and formate dehydrogenases often contain membrane-embedded HydC/FdnI domains that act as menaquinone oxioreductases [24]. In the *G. sulfurreducens* genome, a monocistronic gene [25] referred to here as *cbcL* (c- and *b*-type cytochrome for low potential, GSU0274, sometimes annotated in databases as *cbc*1 or *cbcY* [14]), is predicted to encode an inner membrane HydC/FdnI diheme *b*-type cytochrome linked to a 9-heme periplasmic *c*-type cytochrome (Schematic 1). Homologs are present in genomes of most *Geobacteraceae*, *Acidobacteria*, *Caldithrix* and *Campylobacter*, but this family of putative quinone oxioreductases has never been studied, and lacks an identified function in any of these microorganisms.

To test if CbcL was utilized for respiration by *G. sulfurreducens*, *cbcL* was removed using a markerless deletion protocol. The Δ*cbcL* mutant had no apparent growth defect when fumarate was the electron acceptor, and an only 10% slower doubling time when grown with soluble Fe(III)-citrate as the electron acceptor (Fig. 1A). Reduction of the insoluble electron acceptor Mn(VI)-oxide (birnessite) was also similar to wild type (Fig. 1B). In contrast, when Fe(III)-oxide was the electron acceptor, growth of the Δ*cbcL* mutant was severely impaired. Both the overall rate of Fe(III) reduction and extent after 200 h was less than 30% of wild type cultures (Fig. 1C).

The growth phenotype of the Δ*cbcL* strain was the opposite reported for the Δ*imcH* mutant, which could not reduce Fe(III)-citrate and Mn(IV), yet reduced Fe(III)-oxides at wild type rates. Fe(III)-citrate and Mn(IV)-oxide have relatively high redox potentials (>+0.3 V vs. SHE) [26,27], while the Fe(III)-oxides in these experiments have redox potentials below 0 V. These data suggested the Δ*cbcL* mutant could be specifically impaired in reduction of lower redox potential acceptors. To further test the effect of acceptor potential, the Δ*cbcL* mutant was grown on anodes held at different electron accepting potentials.

3.2. Deletion of cbcL impairs reduction of electrodes poised at lower potential

When electrodes were poised at +0.24 V vs. SHE, the wild type and Δ*cbcL* mutant grew exponentially without lag, with average doubling times of 6.5 ± 0.5 h for wild type and 8.0 ± 0.9 h for the Δ*cbcL* mutant (Fig. 2A, average of 6 experiments, growth rates measured between 12 and 24 h). The Δ*cbcL* mutant achieved 74% of wild type final current density (Fig. 2A, inset). This decrease in final current density was concurrent with a decrease in total protein in the Δ*cbcL* biofilm, indicating that this was primarily due to thinner biofilms layering on electrodes in the final growth stages. This raises the possibility that CbcL becomes more important in thick biofilms, which could develop redox gradients and become more reduced in regions farther from the electrode [28–30].

In contrast, the Δ*cbcL* mutant had a significant growth defect when redox potential was −0.1 V vs. SHE (Fig. 2B). Wild type cells doubled in 8 ± 0.8 h at this redox potential, but the Δ*cbcL* mutant grew poorly, rarely demonstrating doubling times faster than 20 h, and reaching only 14% of the final current density of wild type (Fig. 2B, average of 4 observations). When *cbcL* was expressed from a constitutive promoter in the Δ*cbcL* strain, the complemented

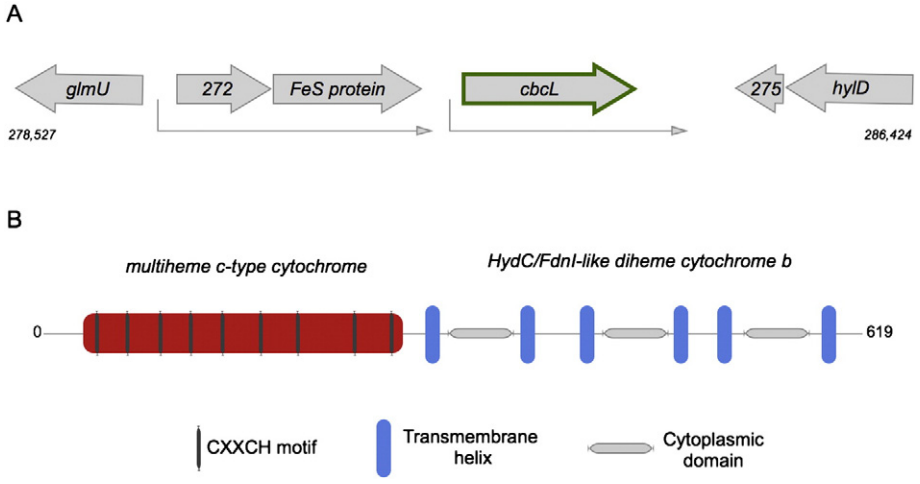

Schematic 1. Genome context and domain structure of *CbcL*. (A) *G. sulfurreducens cbcL* (GSU0274) is monocistronic. In all *Geobacteraceae* genomes, *cbcL* is encoded adjacent to an Fe–S protein, while in *Campylobacter* genomes, the N-terminus includes an Fe–S domain. (B) Predicted features of CbcL include a 9 CXXCH-motif multiheme periplasmic cytochrome, anchored by six inner membrane transmembrane helices. The transmembrane domains are highly similar to diheme *b*-type cytochromes found in menaquinone-dependent formate dehydrogenases.

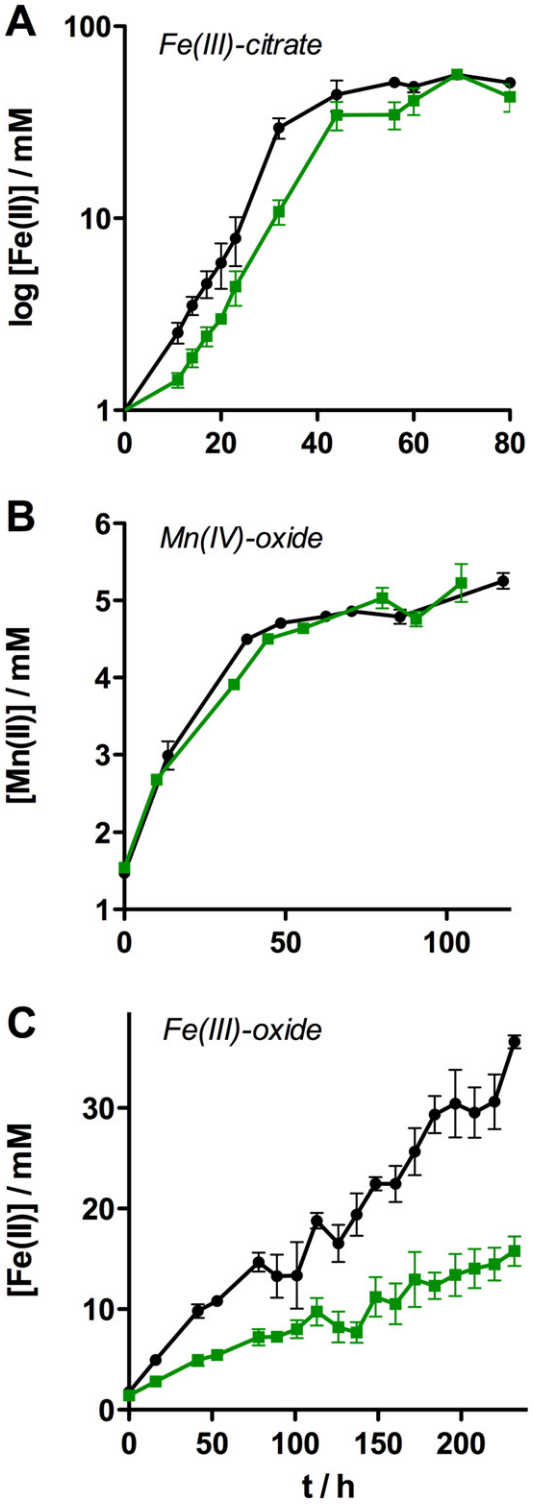

Fig. 1. Metal reduction phenotypes. Growth of wild type (circle, black lines) and Δ*cbcL* (square, green lines) mutants with acetate as the electron donor and different metals as electron acceptors. (A) Soluble Fe(III)-citrate reduction to Fe(II), (B) insoluble Mn(IV)-oxide reduction to Mn(II), and (C) Fe(III)-oxide reduction to Fe(II). Data points are mean ± SD of three replicates.

Δ*cbcL* mutant grew faster, with a doubling time of 12 h, and reached a final current density 2.8-fold higher than the mutant carrying the empty vector alone. This complemented strain was used to further investigate the electrochemical effects of removing and re-expressing *cbcL* in *G. sulfurreducens*.

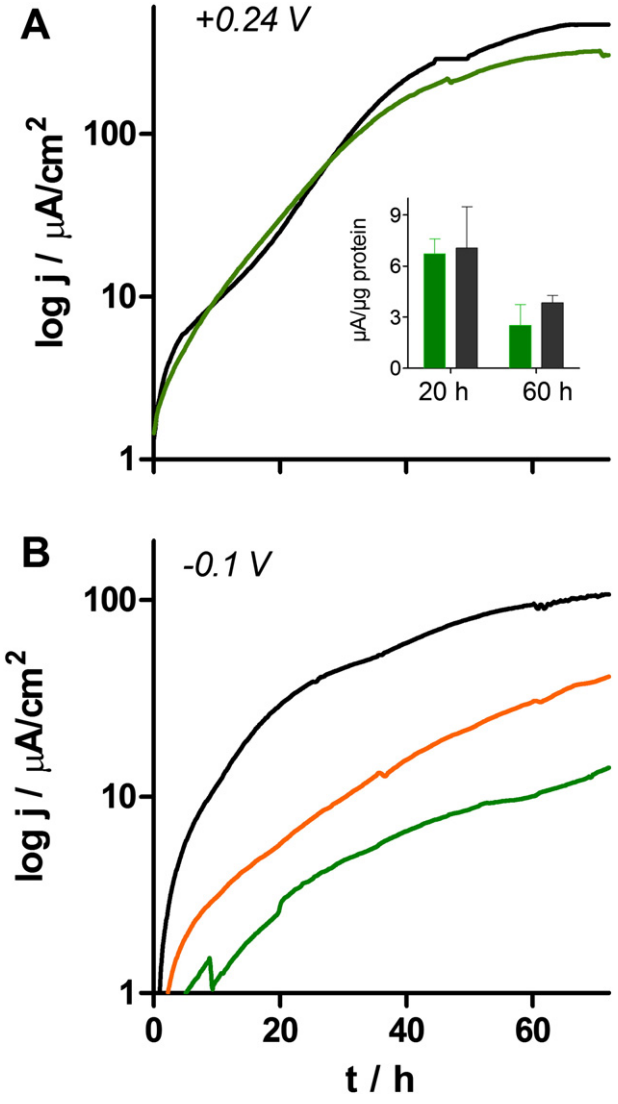

Fig. 2. Growth on electrodes poised at high vs. low redox potentials. Total current density, j, as a function of time on polished graphite electrodes with acetate as the electron donor. (A) High potential growth of wild type (black lines) and Δ*cbcL* (green lines) mutant on a working electrode poised at +0.24 V vs. SHE. Inset: current per unit attached protein at 30 h and 100 h, (values are different at 100 h, $p < 0.05$). (B) Low potential growth of wild type + vector (black), Δ*cbcL* + vector (green), and Δ*cbcL* + p*cbcL* (orange) on a working electrode poised at −0.1 V vs. SHE. All experiments were performed in triplicate, representative traces shown.

3.3. Voltammetry of the ΔcbcL mutant reveals a feature missing at low redox potential

Wild type and mutant biofilms were subjected to catalytic cyclic voltammetry (CV) at 1 mV/s in the presence of acetate as the electron donor (Fig. 3). Wild type biofilms produced a characteristically broad sigmoidal response, with an onset potential of approximately −0.25 V, a midpoint potential of −0.15 V, and a limiting current plateau stabilizing by 0 V. In contrast, the onset of current production by Δ*cbcL* mutants was more positive than wild type. Once initiated, the catalytic wave was steeper, with a midpoint potential of −0.1 V. This indicated that mechanism(s) typically used for electron transfer at lower redox potentials were absent in the Δ*cbcL* mutant. These features were present regardless of the redox potential used to grow cells, and no peaks were observed outside the potential window shown in Fig. 4. Since more robust Δ*cbcL* biofilms could be grown

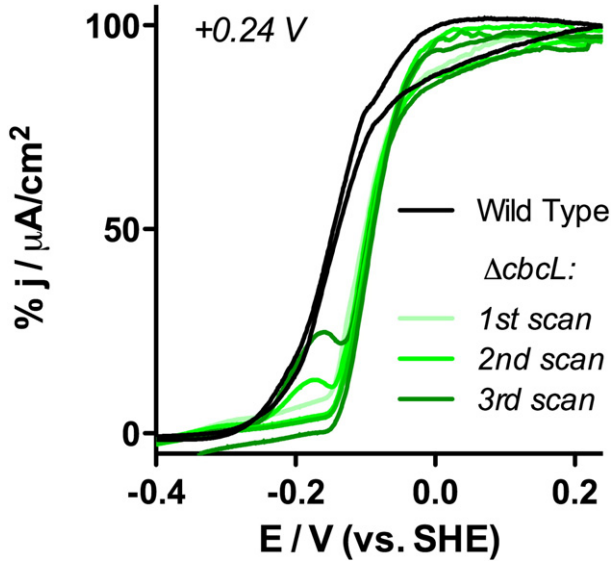

Fig. 3. Shifts in voltammetry due to *cbcL* deletion. After 60 h of growth on working electrodes poised at +0.24 V vs. SHE, 3 cycles at a scan rate of 1 mV/s were performed in the presence of acetate as an electron donor. Data are normalized to the limiting current at +0.2 V. Wild type data (black lines) were similar regardless of scan number, only third scan is shown.

at high potentials, +0.24 V was used as the growth condition for all comparative experiments unless otherwise indicated.

Repeated catalytic voltammetry scans of Δ*cbcL* mutants grown at high potential (+0.24 V) revealed a previously unreported feature. While the first scan contained only the single steep rise, later cycles produced a small anodic peak at approximately −0.2 V. After three full cycles, this feature did not increase in magnitude. This was not observed in wild type biofilms, although it could have easily been obscured by the major processes already present in wild type voltammograms. These results suggested that some electron transfer mechanisms could be activated by exposure to lower redox potentials, such those occurring during voltammetry scans.

When wild type and Δ*cbcL* biofilms were pre-grown at the lower redox potential of −0.1 V, all CV data were similar to 'third scan' data shown in Fig. 3. For example, Δ*cbcL* biofilms already demonstrated the small feature at −0.2 V, and still had positively shifted voltammetry with a midpoint at −0.1 V. As was observed at higher potentials, the major electron transfer process centered at −0.15 V was always absent in the Δ*cbcL* mutant, regardless of growth conditions or redox potential exposure.

When *cbcL* was expressed in the Δ*cbcL* background, voltammetry of the biofilm shifted back towards the lower potential wave characteristic of wild type, and electron transfer at a midpoint potential of −0.15 V could again be detected (Fig. 4A). By plotting the derivative of these voltammograms, three separate midpoint potentials could be identified, with the process at −0.15 V always being dependent upon the presence of *cbcL* (Fig. 4B). Notably, the plasmid used to express *cbcL* only restored 80% of the wild type growth rate, and also only partially restored the voltammetry phenotype. This allowed the peak near −0.15 V to be more easily resolved than in wild type cultures, where the three processes appear as one feature.

Voltammetry of biofilms incubated in the absence of acetate (single-turnover conditions, or non-catalytic) revealed further differences between wild type and Δ*cbcL* mutants (Fig. 4C). Both cultures produced a high-potential reversible peak centered at approximately −0.07 V vs. SHE. However, the Δ*cbcL* mutant biofilm failed to produce many peaks commonly observed at potentials below −0.1 V, even when grown at lower potentials. Unlike turnover conditions where acetate was present, no additional peaks were induced with repeated scanning of Δ*cbcL* biofilms. In the partially complemented strain, peaks in this lower potential domain were restored, particularly cathodic peaks that are characteristic of wild type *G. sulfurreducens*.

3.4. CbcL also contributes to electron transfer at higher potentials

The presence of the CbcL-dependent feature even when cells were grown at high redox potential, and minor wild type growth defects with high potential acceptors suggested that *cbcL* was expressed at both high and low redox potential in wild type cells. According to this hypothesis, *cbcL* is expressed, but somehow not fully active at higher potentials. When quantitative RT-PCR of the *cbcL* mRNA was performed on biofilms grown at +0.24 V and −0.1 V, *cbcL* mRNA was detected under both conditions, and the ratio of *cbcL* mRNA (normalized to *rpoD* levels) at low potential compared to high potential was 1.22 (mean of 3 independent biofilms for each condition). These results were consistent with the slight increase in doubling times observed when Δ*cbcL* mutants utilized high potential metals (Figs. 2 and 3), and the presence of peaks near −0.15 V in single-turnover voltammetry (Fig. 4C) even when WT cells were grown at high potential.

Experiments with electrode-grown biofilms repeatedly show that *Geobacter* catalytic voltammetry fails to conform to a simple Nernstian model in which one redox enzyme is rate-limiting [9,31,32]. A hypothesis for multiple electron transfer pathways in *G. sulfurreducens* was recently described by Yoho et al. [12], based on the improved fit of electrochemical impedance spectroscopy data to a 2-mediator model. The availability of voltammetry from the Δ*cbcL* strain made it possible to observe as many as three rate-limiting steps in *G. sulfurreducens* electron transfer, similar to voltammetry obtained from mixed-*Geobacteraceae* anodes [7].

A variation on the limiting current approach described by Richter et al. [11] ($(i_{max} - i) / i = exp((E - E_o') / (nF/RT))$ was expanded to use the three midpoint potentials (E_o, −0.23, −0.15, and −0.07 V) observed during Δ*cbcL* mutant and complemented strain experiments, to produce a simulation of *G. sulfurreducens* catalytic voltammetry.

In this model, plotted in Fig. 5, i_{max} is the maximum current that can flow through a given inner-membrane pathway, E_o' is the midpoint potential in V, and $n = 1$ for each pathway. The limiting current values for each pathway were chosen by fitting to wild type biofilm voltammograms. Shown in Fig. 5 is the derivative of a simulation, overlaid on the derivative of an actual cathodic scan from a wild type *G. sulfurreducens* biofilm, which was grown for 120 h at +0.24 V to obtain an example of the more complex heterogeneous voltammograms typically studied in these cells. According to this model, the wild type catalytic wave can be described as a result of three pathways with redox potentials spaced roughly 50 mV apart, causing their output to often merge into one broad response.

3.5. Evidence for redox-dependent regulation of electron flux

Interpreted in the simplest way, this model predicts that the CbcL-dependent pathway is responsible for nearly 80% of the flux out of *G. sulfurreducens* cells when an electrode is poised at −0.1 V, which is in agreement with the severe growth inhibition observed when *cbcL* is deleted. However, this model also predicts that the CbcL-dependent pathway could contribute over 60% of electron flux out of cells even when redox potentials rise to +0.24 V. This second prediction is at odds with the fact that mutants containing CbcL, but lacking the ImcH inner membrane cytochrome, are unable to grow at higher potentials. One hypothesis for this behavior is that the CbcL-dependent pathway is significantly restricted from operating when redox potential rises above −0.1 V. This would allow the ImcH-dependent pathway to take over, allowing cells to take advantage of the additional driving force and increase growth rate. According to this model, in Δ*imcH* mutants, the CbcL pathway shuts down as designed at higher redox potentials, and Δ*imcH* cells fail to respire.

A switching of respiratory pathways above −0.1 V is further indicated by voltammograms of *Geobacter*, such as those in Fig. 4. Rather than a smooth handoff from the process centered at −0.15 V to those at higher potential, voltammograms typically reflect a sharp drop and recovery

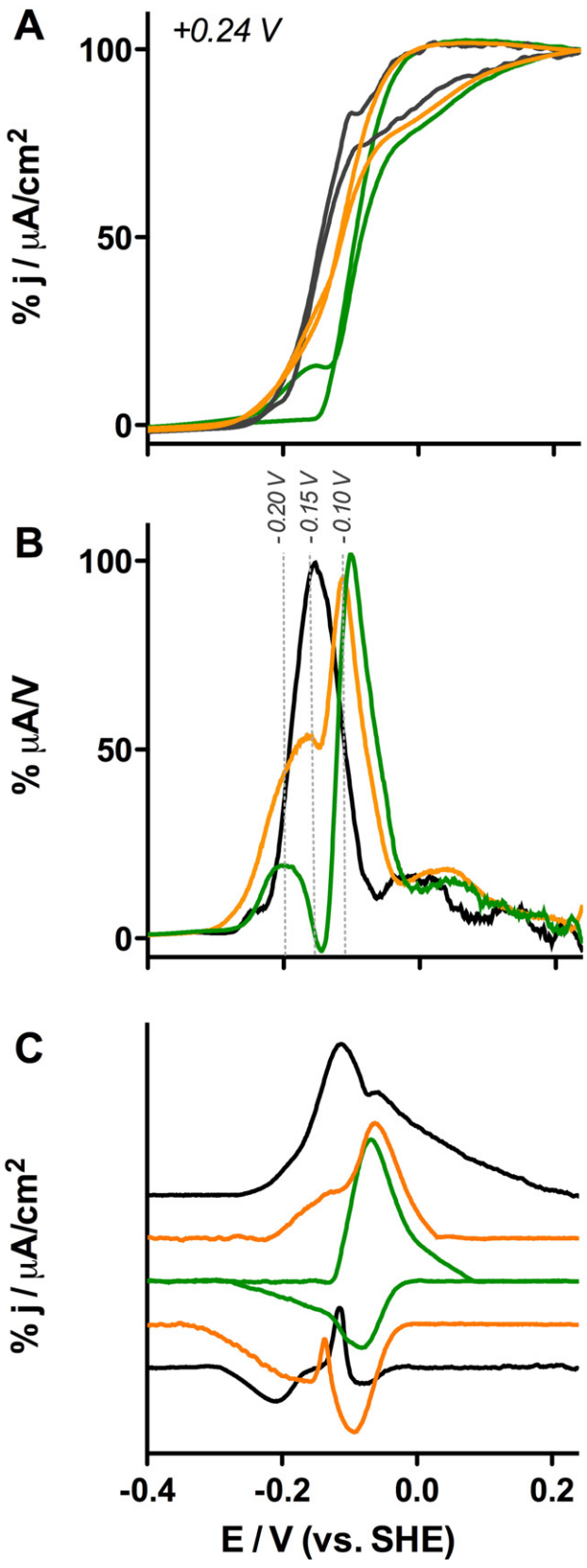

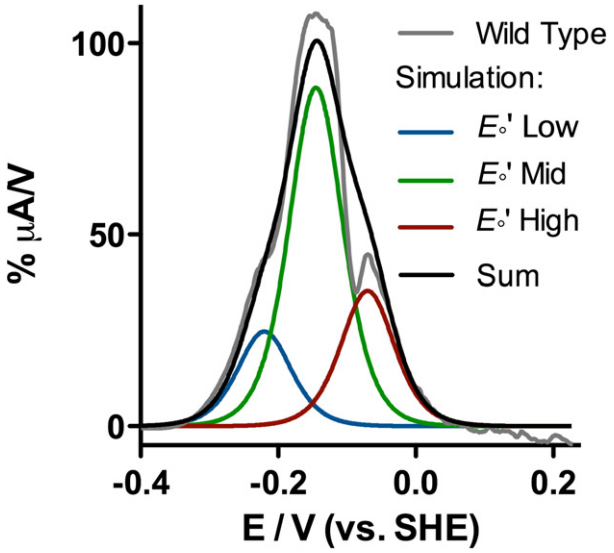

Fig. 5. Comparison of wild type voltammetry to a 3-site model. Gray line is the derivative from a cathodic sweep of a fully grown, 120-h old biofilm. Using the equation generated by Richter et al. [10], derivatives of three different catalytic waves are indicated, with the "Low" midpoint at −0.23 V vs. SHE, "Mid" at −0.15 V and "High" at −0.07 V. The sum of these three catalytic waves is shown by the bold line for comparison to the wild type biofilm scanned at 1 mV/s.

that deviates from any model prediction. A similar event occurs in the same region of single-turnover voltammograms; a sharp unexplained cathodic peak near −0.1 V. This behavior disappears when *cbcL* is deleted (Fig. 4C). The fact that both *imcH* and *cbcL* are constitutively expressed, and are possibly post-transcriptionally regulated via unknown redox potential-dependent interactions, may also explain why earlier proteomic and transcriptomic studies did not draw attention to these proteins [16,33].

3.6. Implications for anode growth and analysis of microbial voltammetry

While electrochemical techniques yield useful response curves from bacteria undergoing extracellular respiration, an explanation for the nonstandard sigmoidal voltammogram has remained elusive. Outer membrane redox proteins, or electron transfer at the electrode interface, could govern these features. Based on analogies to redox polymers, many conceptual models of microbial electron transfer invoke a rate-limiting 'mediator' step on the cell exterior with a single diagnostic midpoint potential. However, most analyses of anode bacteria conclude that voltammetry is inconsistent with interfacial electron transfer reactions being slow [9], and that the midpoint potentials of mediators catalyzing between-cell electron transfer are lower than the midpoint potentials that govern catalytic voltammetry [30].

If outer membrane or interfacial electron transfer is not rate-limiting, then catalytic voltammetry does not reflect the mechanism of interfacial electron transfer per se. Analogous to protein film voltammetry, electron flow between surfaces and proteins, and electron transfer between redox cofactor networks, are easily reversible in *Geobacter*. It is more likely that the reaction with a significant ΔG, the exit of electrons

Fig. 4. Cyclic voltammetry of complemented mutants. After 60 h of growth on working electrodes poised at +0.24 V vs. SHE, 3 cycles at a scan rate of 1 mV/s were performed in the presence of acetate as an electron donor, third scan is shown normalized to the limiting current at +0.2 V. (A) Wild type with empty vector (black lines), Δ*cbcL* expressing *cbcL* (orange lines) and Δ*cbcL* with empty vector (green lines) control cyclic voltammetry, (B) first derivative of data in (A), showing the presence of a process in the complemented strain that is absent in the Δ*cbcL* mutant, (C) non-catalytic cyclic voltammetry of wild type, complemented and Δ*cbcL* biofilms in the absence of acetate. Each data set is normalized to the highest peak and baseline subtracted.

from the inner membrane linked to proton motive force generation, controls the kinetics of *Geobacter* respiration.

These results provide a warning that subtle redox potential differences can affect the growth of pure cultures or communities enriched from the environment. Changes in acceptor potential, such as from 0 V to −0.1 V vs. SHE, are enough to switch *G. sulfurreducens* between two electron transfer pathways. These changes can manifest as longer doubling times and smaller biofilms on electrodes. Studies demonstrating similar redox potential effects at this resolution are emerging, such as by Commault et al. [7], Yoho et al. [12], and Rose et al. [34].

4. Conclusions

There is mounting evidence for at least two electron transfer pathways out of the *G. sulfurreducens* inner membrane, that are used in reduction of distant acceptors with distinct redox potentials. These results have implications in energy-generating devices such as microbial fuel cells, as the pathways that operate at the lowest anode potentials are those revealed by CbcL-like proteins. The existence of multiple pathways also suggests that electron transfer to freshly precipitated high-potential FeOOH requires different proteins than low potential Goethite or $UO_2(CO_3)_2^{=}$. Syntrophic interspecies electron transfer may also require the donor organism to utilize a low potential strategy [17]. Thus, redox potential must be carefully controlled and considered in the study of extracellular respiration. Regardless of where an electron ultimately travels, a respiratory bacterium must first confront the reality of thermodynamics at the inner membrane.

Acknowledgments

L.Z. and D.R.B. were supported by U.S. Department of Energy, DE-SC0006868. C.H.C. and D.R.B. were supported by the Office of Naval Research, N0001410308.

Appendix A. Supplementary data

Supplementary data to this article can be found online at http://dx.doi.org/10.1016/j.bioelechem.2015.08.003.

References

[1] K.A. Weber, M.M. Urrutia, P.F. Churchill, R.K. Kukkadapu, E.E. Roden, Anaerobic redox cycling of iron by freshwater sediment microorganisms, Environ. Microbiol. 8 (2005) 100–113.
[2] M. Blöthe, E.E. Roden, Microbial iron redox cycling in a circumneutral-pH groundwater seep, Appl. Environ. Microbiol. 75 (2009) 468–473.
[3] J. Simon, R.J.M. van Spanning, D.J. Richardson, The organisation of proton motive and non-proton motive redox loops in prokaryotic respiratory systems, Biochim. Biophys. Acta 1777 (2008) 1480–1490.
[4] E.C. Salas, W.M. Berelson, D.E. Hammond, A.R. Kampf, K.H. Nealson, The impact of bacterial strain on the products of dissimilatory iron reduction, Geochim. Cosmochim. Acta 74 (2011) 574–583.
[5] J. Majzlan, Minerals and aqueous species of iron and manganese as reactants and products of microbial metal respiration, in: J. Gescher, A. Kappler (Eds.), Microb. Met. Respir. from Geochemistry to Potential Applications, 1st ed.Springer Verlag, New York, NY 2012, pp. 112–128.
[6] X. Zhu, M.D. Yates, M.C. Hatzell, H.A. Rao, P.E. Saikaly, B.E. Logan, Microbial community composition is unaffected by anode potential, Environ. Sci. Technol. (2014) 1352–1358.
[7] A.S. Commault, G. Lear, M.A. Packer, R.J. Weld, Influence of anode potentials on selection of *Geobacter* strains in microbial electrolysis cells, Bioresour. Technol. 139 (2013) 226–234.
[8] S. Ishii, S. Suzuki, T.M. Norden-Krichmar, A. Tenney, P.S.G. Chain, M.B. Scholz, K. Nealson, O. Bretschger, A novel metatranscriptomic approach to identify gene expression dynamics during extracellular electron transfer, Nat. Commun. 4 (1841) 1601.
[9] M. Rimboud, E. Desmond-Le Quemener, B. Erable, T. Bouchez, A. Bergel, Multi-system Nernst–Michaelis–Menten model applied to bioanodes formed from sewage sludge, Bioresour. Technol. 195 (2015) 192-169.
[10] S.M. Strycharz, A.P. Malanoski, R.M. Snider, H. Yi, D.R. Lovley, L.M. Tender, Application of cyclic voltammetry to investigate enhanced catalytic current generation by biofilm-modified anodes of *Geobacter sulfurreducens* strain DL1 vs. variant strain KN400, Energy Environ. Sci. 4 (2011) 896–913.
[11] H. Richter, K.P. Nevin, H. Jia, D.A. Lowy, D.R. Lovley, L.M. Tender, Cyclic voltammetry of biofilms of wild type and mutant *Geobacter sulfurreducens* on fuel cell anodes indicates possible roles of OmcB, OmcZ, type IV pili, and protons in extracellular electron transfer, Energy Environ. Sci. 2 (2009) 506–516.
[12] R.A. Yoho, S.C. Popat, C.I. Torres, Dynamic potential-dependent electron transport pathway shifts in anode biofilms of *Geobacter sulfurreducens*, ChemSusChem (2014) 3413–3419.
[13] C.E. Levar, C.H. Chan, M.G. Mehta-kolte, D.R. Bond, An inner membrane cytochrome required only for reduction of high redox potential extracellular electron acceptors, MBio 5 (6) (2014) 1–9.
[14] J.E. Butler, N.D. Young, D.R. Lovley, Evolution of electron transfer out of the cell: comparative genomics of six *Geobacter* genomes, BMC Genomics 11 (2010) 40.
[15] M. Aklujkar, M.V. Coppi, C. Leang, B.C. Kim, M.A. Chavan, L.A. Perpetua, L. Giloteaux, A. Liu, D.E. Holmes, Proteins involved in electron transfer to Fe(III) and Mn(IV) oxides by *Geobacter sulfurreducens* and *Geobacter uraniireducens*, Microbiology 159 (2013) 515–535.
[16] Y.-H.R. Ding, K.K. Hixson, M.A. Aklujkar, M.S. Lipton, R.D. Smith, D.R. Lovley, T. Mester, Proteome of *Geobacter sulfurreducens* grown with Fe(III) oxide or Fe(III) citrate as the electron acceptor, Biochim. Biophys. Acta 1784 (2008) 1935–1941.
[17] P.M. Shrestha, A.-E. Rotaru, M. Aklujkar, F. Liu, M. Shrestha, Z.M. Summers, et al., Syntrophic growth with direct interspecies electron transfer as the primary mechanism for energy exchange, Environ. Microbiol. Rep. 5 (2013) 904–910.
[18] S. Ishii, S. Suzuki, T.M. Norden-Krichmar, T. Phan, G. Wanger, K.H. Nealson, Y. Sekiguchi, Y. Gorby, O. Bretschger, Microbial population and functional dynamics associated with surface potential and carbon metabolism, ISME J. 8 (2014) 963–978.
[19] E. Marsili, J.B. Rollefson, D.B. Baron, R.M. Hozalski, D.R. Bond, Microbial biofilm voltammetry: direct electrochemical characterization of catalytic electrode-attached biofilms, Appl. Environ. Microbiol. 74 (2008) 7329–7337.
[20] D.R. Lovley, E.J.P. Phillips, Organic matter mineralization with reduction of ferric Iron in anaerobic sediments organic matter mineralization with reduction of ferric iron in anaerobic sediments, Appl. Environ. Microbiol. 51 (1986) 683–689.
[21] A. Schafer, A. Tauch, W. Jager, J. Kalinowski, G. Thierbach, A. Puhler, Small mobilizable multi-purpose cloning vectors derived from the *Escherichia coli* plasmids pK18 and pK19: selection of defined deletions in the chromosome of *Corynebacterium glutumicum*, Gene 145 (1994) 69–73.
[22] A. Simon, R. Priefer, U. Puhler, A broad host range mobilization system for *in vivo* genetic engineering: transposon mutagensis in gram negative bacteria, Biotechnology 1 (1983) 784–791.
[23] S. Fleige, M.W. Pfaffl, RNA integrity and the effect on the real-time qRT-PCR performance, Mol. Aspects Med. 27 (2006) 126–139.
[24] M. Jormakka, S. Tornroth, B. Byrne, S. Iwata, Molecular basis of proton motive force generation: structure of formate dehydrogenase-N, Science 295 (2002) 1863–1868.
[25] Y. Qiu, B.-K. Cho, Y.S. Park, D. Lovley, B.Ø. Palsson, K. Zengler, Structural and operational complexity of the *Geobacter sulfurreducens* genome, Genome Res. 20 (2010) 1304–1311.
[26] K.L. Straub, M. Hanzlik, B.E. Buchholz-Cleven, The use of biologically produced ferrihydrite for the isolation of novel iron-reducing bacteria, Syst. Appl. Microbiol. 21 (1998) 442–449.
[27] K.L. Straub, B. Schink, Ferrihydrite reduction by *Geobacter* species is stimulated by secondary bacteria, Arch. Microbiol. 182 (2004) 175–181.
[28] B. Virdis, D. Millo, B.C. Donose, D.J. Batstone, Real-time measurements of the redox states of c-type cytochromes in electroactive biofilms: a confocal resonance raman microscopy study, PLoS One 9 (2014) e89918.
[29] B. Virdis, F. Harnisch, D.J. Batstone, K. Rabaey, B.C. Donose, Non-invasive characterization of electrochemically active microbial biofilms using confocal Raman microscopy, Energy Environ. Sci. 5 (2012) 7017–7024.
[30] R.M. Snider, S.M. Strycharz-Glaven, S.D. Tsoi, J.S. Erickson, L.M. Tender, Long-range electron transport in *Geobacter sulfurreducens* biofilms is redox gradient-driven, Proc. Natl. Acad. Sci. U. S. A. 109 (2012) 15467–15472.
[31] C.I. Torres, A. Kato Marcus, B.E. Rittmann, Proton transport inside the biofilm limits electrical current generation by anode-respiring bacteria, Biotechnol. Bioeng. 100 (2008) 872–881.
[32] H.V.M. Hamelers, A. Ter Heijne, N. Stein, R.a. Rozendal, C.J.N. Buisman, Butler–Volmer–Monod model for describing bio-anode polarization curves, Bioresour. Technol. 102 (2011) 381–387.
[33] E.D. Merkley, K. Wrighton, C.J. Castelle, B.J. Anderson, M.J. Wilkins, V. Shah, et al., Changes in protein expression across laboratory and field experiments in *Geobacter bemidjiensis*, J. Proteome Res. (2014) 1361–1375.
[34] N.D. Rose, J.M. Regan, Changes in phosphorylation of adenosine phosphate and redox state of nicotinamide–adenine dinucleotide (phosphate) in *Geobacter sulfurreducens* in response to electron acceptor and anode potential variation, Bioelectrochemistry 106 (2015) 213–220.